Simultaneous Determination of Dopamine and Tyrosine Using Poly-glycine/Nafion/MWCNTs Functionalized Plastic-based Miniature Electrochemical Platform

Hui Yang[*], Zhiqiang Wei, Ting Li, Liuyang Cheng, Yuanhui Li, Xue Zhang, Wenke Li, Yile Hu[*]

College of Medical, Henan University of Science and Technology, Luoyang, 471023, China.
[*]E-mail: yanghui7761@163.com, huyile2@163.com.

In this study, a novel, simple, low cost and reproducible method is developed to fabricate plastic-based miniature electrochemical platform (PMEP), which integrated three electrodes including a polyglycine/Nafion/MWCNTs modified carbon paste electrode (p-Gly/Nafion/MWCNTs/CPE), a Pt wire counter electrode (CE) and an Ag/AgCl wire reference electrode (RE). The p-Gly/Nafion/MWCNTs/CPE is prepared by drop-coating and in situ electrochemical polymeric deposition. The p-Gly/Nafion/MWCNTs functionalized PMEP (p-Gly/Nafion/MWCNTs/CPE-PMEP) demonstrates excellent electrocatalytic properties for the oxidation of dopamine (DA) and tyrosine (Tyr). Under the optimum conditions, the peak currents of DA and Tyr increase linearly with their concentrations in the ranges of 0.025-10 μM DA and 0.2-40 μM Tyr. And the detection limits (S/N=3) are 0.008 μM and 0.07 μM, respectively. Furthermore, the proposed p-Gly/Nafion/MWCNTs/CPE-PMEP is applied to simultaneous determination of DA and Tyr in human serum samples.

1. INTRODUCTION

The occurrence and prognosis of many diseases are related to the variations of various molecules at metabolic level. Therefore, it is significant to develop low cost and easy to use miniaturized detection devices to meet the patient's needs [1]. Electrochemical technique has unique advantages in promoting the miniaturization and integration of detection platform [2]. In recent years, plastic-based miniature electrochemical platform (PMEP) has established assorted formats according to different applications in analytical research [3]. In addition to pollution prevention and cost reduction, PMEP also improves the efficiency of analysis [4].

Dopamine (4-(2-aminoethyl) benzene-1, 2-diol, DA) is a kind of catecholamine, and it is also a

vital neurotransmitter involved in cognitive function [5]. It has been proved that neurological disorders including Parkinson's disease [6], Schizophrenia [7] and Tourette's syndrome [8] are caused by the unusual level of dopamine. Tyrosine (4-hydroxyphenylalanine, Tyr) is the precursor of catecholamine (dopamine, norepinephrine, and epinephrine) synthesis [9]. It plays an important role in various biological processes. The failure in the metabolic pathway will lead to some inherited diseases, such as tyrosinemia [10] and phenylketonuria [11], and also affect the balance of dopamine [12]. Thus, an accurate, rapid and sensitive method for simultaneous determination of DA and Tyr is of great significance for point of care test (POCT).

The POCT of DA or Tyr in body fluids is challenging because of their low concentrations. Many traditional methods for the determination of DA or Tyr have been developed, such as high performance liquid chromatography [13-14], capillary electrophoresis [15-16] and HPLC-mass spectrometry [17-18]. Although these methods can detect DA or Tyr, they require tedious pretreatment, long-time working, special instruments and high cost. In contrast, electrochemical methods have the advantages of high sensitivity, low cost, easy operation and real-time response [19].

In order to improve electrochemical response, chemical modification electrodes have been widely employed in the past decade [20-23]. MWCNTs (multi-wall carbon nanotubes) are excellent electrode modified materials because of their unique structure and properties, such as good conductivity, high electrocatalytic effect and strong adsorption capacity [24]. Nafion, a cation-exchanger polymer and dispersant, which is often used as electrode modification material [25]. Polyglycine (p-Gly) can be prepared by electrochemical polymerization of glycine, and it provides a larger specific surface area by forming uniform membranes and improves the electron transfer rate through the strong adhesion between the polymer and the electrode surface [26].

In this study, we report a new method for fabricating PMEP by electrochemical modification and micromachining technology. The p-Gly/Nafion/MWCNTs modified carbon paste electrode (p-Gly/Nafion/MWCNTs/CPE) is prepared by the combination of MWCNTs, Nafion and p-Gly. The prepared p-Gly/Nafion/MWCNTs/CPE-PMEP can be used for efficient, inexpensive, time-saving and simultaneous detection of DA and Tyr in human serum samples.

2. EXPERIMENTAL

2.1 Reagents

All reagents were analytical grade. Dopamine, tyrosine and glycine were obtained from Sigma-aldrich (Shanghai, China). Acetic acid, boric acid, phosphoric acid, graphite powder, paraffin oil, sodium hydroxide, dipotassium hydrogen phosphate and potassium dihydrogen phosphate were purchased from Sinopharm Chemical Reagent (Shanghai, China). Nafion (0.5% in ethanol, w/w) was acquired from Cool chemistry (Beijing, China). Multi-walled carbon nanotubes, with purity > 97%, length < 2μm and inner diameter of 10-20 nm, were obtained from Nanotech Port (Shenzhen, China). All solutions were prepared with ultrapure water (Millipore, USA).

2.2 Apparatus

All Electrochemical experiments were performed using CHI 660E electrochemical analyzer equipped with data processing software (CH Instrument, Shanghai, China). The p-Gly/nafion/MWCNTs/CPE-PMEP was employed all through the experiments. The pH measurements were performed with a pHS-3C digital pH meter (INESA Scientific Instrument, Shanghai, China). Scanning electron microscope (SEM) characterizations were performed by focused ion beam scanning electron microscopy (Auriga FIB SEM, Carl Zeiss, Germany) at the desired magnification. Raman spectra characterizations were performed with Laser Raman Spectrometer (LabRAM HR Evolution, HORIBA, France) in the wave number range of 1000-2000 cm^{-1} with 633 nm excitation wavelength.

2.3 Fabrication of CPE-PMEPs

Transparent polymethyl methacrylate (PMMA) plastic plate (thickness: 0.5 mm) was selected for PMEP fabrication. Plastic plate was made into the *components (1(A) I, II and III)* by mechanical micro-engraving technology according to the required dimensions indicated in Fig. 1A. The copper film (thickness: 20μm), which acts as a conductor of CPE, was covered on the surface of *component 1(A) I*. A round hole (diameter: 4 mm) was located at the right-center position of *component 1(A) II* as the mould of CPE. *Component 1(A) III* also had a round hole (diameter: 6 mm), which matches the center of the circular hole of *component 1(A) II,* acted as the electrochemical detection cell. And there was a pair of U-shaped grooves on both sides of the round hole of *component 1(A) III* for fixing Pt wire counter electrode (CE, diameter: 0.2 mm) and Ag/AgCl wire reference electrode (RE, diameter: 0.2 mm).

The fabrication of p-Gly/Nafion/MWCNTs/CPE-PMEP was shown in Fig. 1B. Firstly, *component 1(A) I* and *component 1(A) II* were glued by α-cyanoacrylate adhesive (Fig. 1B I), and 0.2 g graphite powder and 100 μL paraffin oil were mixed to a homogeneous paste in a mortar. Then the resulting homogeneous paste was filled into the hole of *component 1(B) I* and scraped flat using a glass microscope slide to make CPE (*component 1(B) II*). Secondly, MWCNTs were purified according to the literature methods [27], and 20 μl Nafion solution (0.1% in ethanol, w/w) containing 0.2 mg purified MWCNTs was dropped onto the *component 1(B) II*. After standing for 6 h at 25 °C, Nafion/MWCNTs modified CPE (*component 1(B) III*) was fabricated. Next, *component 1(A) III*，*component 1(A)IV* and *component 1(B)III* were assembled to form Nafion/MWCNTs/CPE-PMEP as shown in Fig. 1B IV. Finally, p-Gly/Nafion/MWCNTs/CPE-PMEP was fabricated by dropping 60 μL15 mM glycine solution (0.1 M PBS, pH 6.0) into the detection cell, and cyclic scans were executed by applying 10 consecutive cycles in the range of -0.40 to +1.85 V (*vs.* Ag/AgCl) with initial potential of -0.40 V at scan rate of 100 mV·s^{-1} (Fig. 1B V) [28]. Fig. 1C and Fig. 1D shown schematic illustration of p-Gly/Nafion/MWCNTs sensing interface and the photograph of p-Gly/Nafion/MWCNTs/CPE-PMEP, respectively.
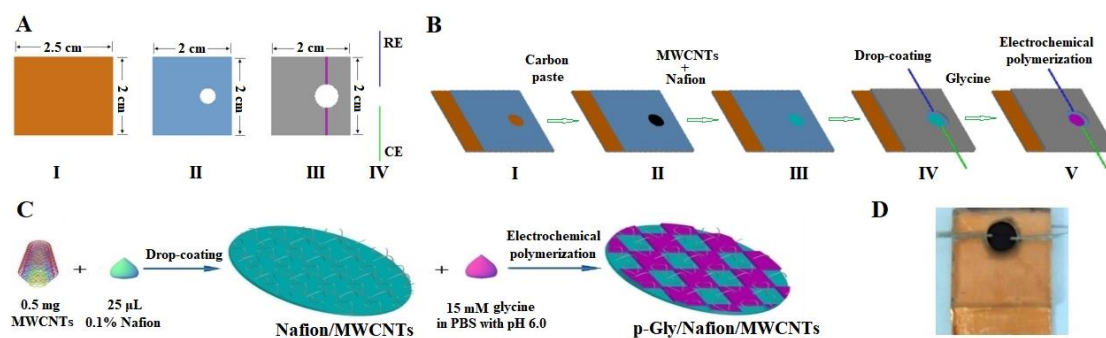
Figure 1. (A). Schematic illustrations of the components. Copper film covered plastic plate (I); Plastic plate with a round hole (II); Plastic plate with a round hole and a pair of U-shaped grooves (III); Pt wire (CE) and Ag/AgCl wire (RE) (IV). (B). Schematic illustration of p-Gly/Nafion/MWCNTs/CPE-PMEP fabrication. *Component 1(A) I* and *component 1(A) II* were glued (I); bare CPE (II); Nafion/MWCNTs/CPE (III); Gly/Nafion/MWCNTs/CPE (IV); p-Gly/Nafion/MWCNTs/CPE-PMEP (V). (C). Schematic illustration of p-Gly/Nafion/MWCNTs sensing interface. (D). Photograph of p-Gly/Nafion/MWCNTs/CPE-PMEP.

2.4 Electrochemical measurements

Stock solution of DA and Tyr were prepared in Britton-Robinson buffer solution (BRBS) (pH 2.0). Different concentrations of DA and Tyr solutions were prepared by diluting the stock solution with buffer solution.

Linear sweep voltammetry (LSV) were carried out for the electrochemical detection of DA and Tyr at bare CPE-PMEP or modified CPE-PMEPs by applying potential from +0.1 to +1.1 V (*vs.* Ag/AgCl) with initial potential of +0.1 V at scan rate of 50 mV·s⁻¹ in BRBS. The test solutions were thoroughly purged with nitrogen before experiments. All electrochemical measurements were performed at room temperature.

2.5 Sample preparation

The human serum sample was obtained from Henan University of Science and Technology First Affiliated Hospital, and stored at 4 °C when not in use. The serum was diluted 10 times with BRBS (pH 5.0) without any pretreatment. The concentrations of DA and Tyr in human serum were determined by standard addition method.

3. RESULTS AND DISCUSSION

3.1 Characterization of p-Gly/Nafion/MWCNTs composite material

SEM images of Nafion/MWCNTs and p-Gly/Nafion/MWCNTs were shown in Fig. 2. Although the nafion film has some influence, the typical carbon nanotube structure can still be observed (Fig. 2a). The structure of p-Gly/Nafion/MWCNTs is coarser, and the typical structure of

MWCNTs becomes blurred (Fig. 2b). This results shown that the morphology of p-Gly/Nafion/MWCNTs sensing interface is different from Nafion/MWCNTs sensing interface after electro-polymerization of Gly on the surface of Nafion/ MWCNTs composite material.
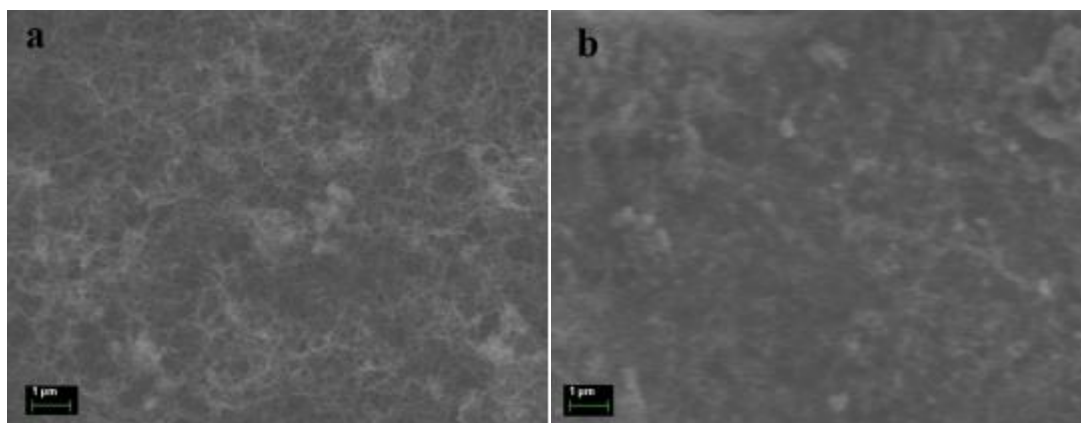
Figure 2. SEM images of Nafion/MWCNTs sensing interface (a) and p-Gly/Nafion/MWCNTs sensing interface (b).

The Raman spectrogram of Nafion/MWCNTs sensing interface shown that there were two bands at 1321 and 1573 cm^{-1} (Fig. 3a), representing the D and G band of carbon based materials. And the two characteristic bands were at 1319 and 1578 cm^{-1} in the Raman spectrogram of p-Gly/Nafion/MWCNTs sensing interface (Fig. 3b). Moreover, the intensity ratio of I_D/I_G of p-Gly/Nafion/MWCNTs sensing interface (1.02) was slightly smaller than that of Nafion/MWCNTs sensing interface (1.06), indicating that the randomness of p-Gly/Nafion/MWCNTs sensing interface remains unchanged [29].
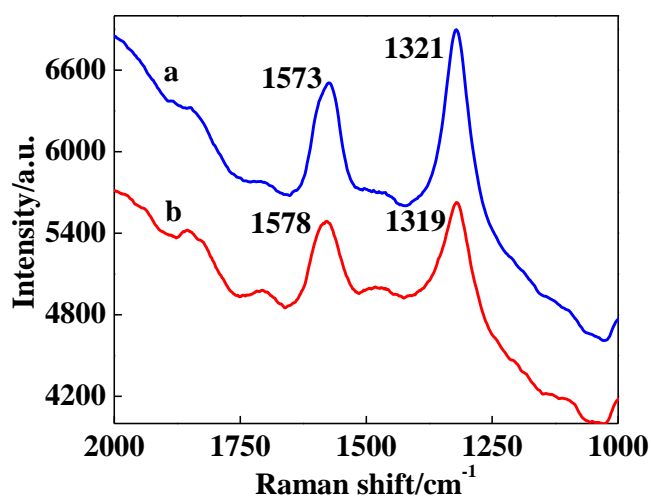
Figure 3. Raman spectrograms of Nafion/MWCNTs sensing interface (a) and p-Gly/Nafion/MWCNTs sensing interface (b).

3.2 Electrochemical characterization of bare CPE-PMEP and
modified p-Gly/Nafion/MWCNTs/CPE-PMEPs

In order to explore the electrochemical performance of bare CPE-PMEP and modified p-Gly/Nafion/MWCNTs/CPE-PMEPs, the external redox probe $[Fe(CN)_6]^{3-/4-}$ had been studied by cyclic voltammetry (CV). As shown in Fig. 4(A), the oxidation peak current of p-Gly/Nafion/MWCNTs/CPE-PMEP increases from 32.2 µA to 63.1 µA. Meanwhile, the oxidation peak potential decreased from +0.217 V to +0.156 V, indicating that p-Gly/Nafion/MWCNTs promoted the electron transfer between the electrode and solution. As shown in Fig. 4(B), the peak currents increased with the increase of potential scan rates and were linearly correlated with the square root of the scan rates in the range of 10-150 $mV \cdot s^{-1}$, indicating the diffusion controlled process on the electrode surface.
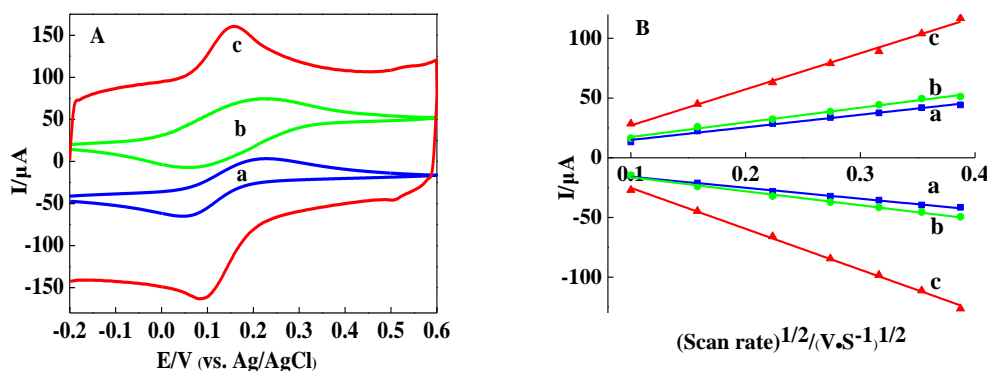
Figure 4. (A) CV curves of bare CPE-PMEP (a), Nafion/MWCNTs/CPE-PMEP (b) and p-Gly/Nafion/MWCNTs/CPE-PMEP (c) in 0.1 M KCl containing 2.0×10^{-4} M $[Fe(CN)_6]^{3-/4-}$. (B) CV peak current analysis of bare CPE-PMEP (a), Nafion/MWCNTs/CPE-PMEP (b) and p-Gly/Nafion/MWCNTs/CPE-PMEP (c) at various scan rates (10-150 $mV \cdot s^{-1}$).

CVs were carried out for further investigating the electrochemical behaviors of p-Gly/Nafion/MWCNTs/CPE-PMEP in BRBS (pH 5.0) containing DA and Tyr. As shown in Fig.5(A), p-Gly/Nafion/MWCNTs/CPE-PMEP showed remarkable efficient electrocatalytic activity for the oxidation of DA and Tyr. DA has obvious reduction peak, while the reduction peak of Tyr has not been observed. The oxidation peak potentials of DA and Tyr were located at +0.43 V and +0.87 V, respectively. The potential separation between DA and Tyr oxidation peaks was 440 mV. Therefore, it was feasible for simultaneous electrochemical determination of DA and Tyr on p-Gly/Nafion/MWCNTs/CPE-PMEP.
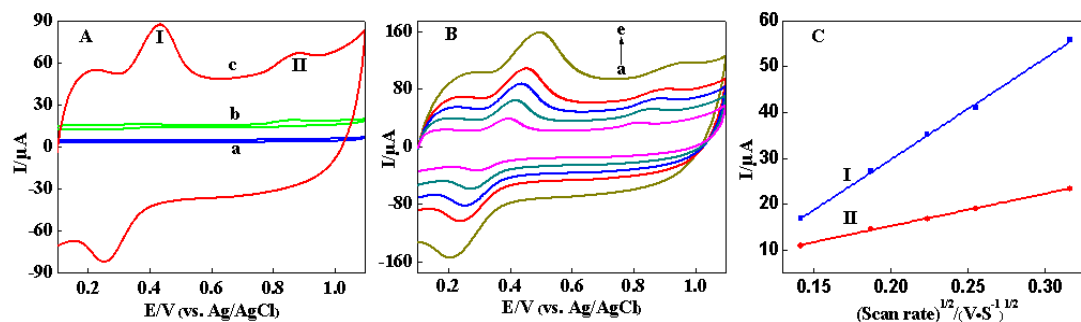
Figure 5. (A) CV curves of DA and Tyr at bare CPE-PMEP (a), Nafion/MWCNTs /CPE-PMEP (b) and p-Gly/Nafion/MWCNTs CPE-PMEP (c), scan rate: 50 mV·s⁻¹. (B) CV curves of DA and Tyr at p-Gly/Nafion/MWCNTs/CPE-PMEP at different CV scan rates (a→e: 10-100 mV·s⁻¹). (C) The linear relationship of current and the square root of the scan rate. I: 10 μM DA, II: 30 μM Tyr. Buffer solution: BRBS (pH 5.0).

Fig. 5B showed that oxidation peak currents of DA and Tyr increased with the scan rate increasing. The relationship of current and the square root of scan rate was found to be linear: $I_{pa, DA}$ (μA) = 220.59 μA $(V·s^{-1})^{1/2}$ - 14.364 μA, R^2 = 0.997; $I_{pa, Try}$ (μA) = 70.366 μA $(V·s^{-1})^{1/2}$ + 1.134 μA, R^2 = 0.998) (Fig. 5C). Therefore, these indicate that the electrochemical behaviors of DA and Tyr at p-Gly/Nafion/MWCNTs/CPE-PMEP are diffusion-controlled [30].

3.3 Influence of detection buffer solution pH

Because the protons are involved in the electrode reaction of DA and Tyr, pH value of buffer solution is very important for detection of DA and Tyr [31]. So, the oxidation potentials and current responses of DA and Tyr at p-Gly/Nafion/MWCNTs/CPE-PMEP were investigated in BRBS with different pH value. As shown in Fig. 6A and Fig. 6B, the oxidation potential of DA increased firstly and then decreased, and the maximum of the oxidation peak current was observed at pH 5.0. In comparison, though the oxidation potential of Tyr also varied with the increase of pH value, there is very little change of the oxidation peak current. Therefore, pH 5.0 was chosen as an optimum solution pH for further experiments. As shown in Fig. 6C, the oxidation potential of DA and Tyr decreased with the pH value increasing, and the relationships between the potentials and pH were linear: $E_{pa, DA}$ (V) = 0.7732 - 0.0694 pH, R^2 =0.998; $E_{pa, Tyr}$ (V) =1.1204 - 0.0494 pH, R^2 =0.995. The slope of the equation is -59 mV, which is close to the Nernstian value of the electrochemical process of the same number of protons and electrons [32]. The oxidation-reduction mechanism for DA and Tyr at p-Gly/Nafion/MWCNTs/CPE-PMEP was shown in Scheme 1.
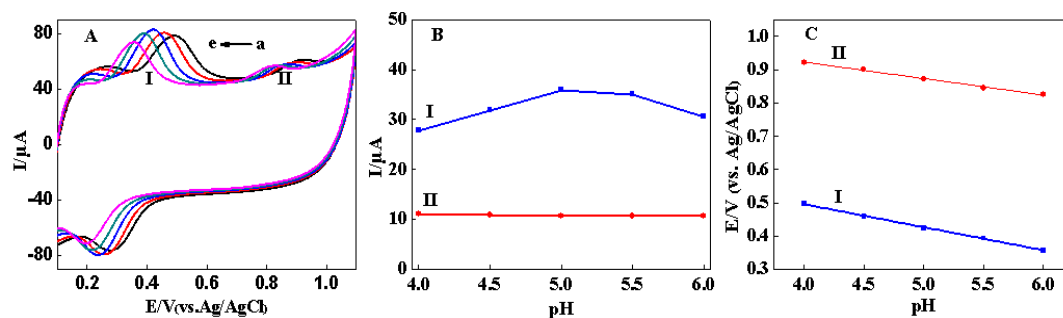
Figure 6. (A) CV curves obtained at p-Gly/Nafion/MWCNTs/CPE-PMEP in BRBS with different pH value (a→e: pH 4.0-6.0). (B) Influence of pH value on the current response of DA and Tyr at p-Gly/Nafion/MWCNTs/CPE-PMEP. (C) The plots of anodic peak potential (E_{pa}) of DA and Tyr versus pH values. I: 10 μM DA, II: 30 μM Tyr. Scan rate: 50 mV·s^{-1}.
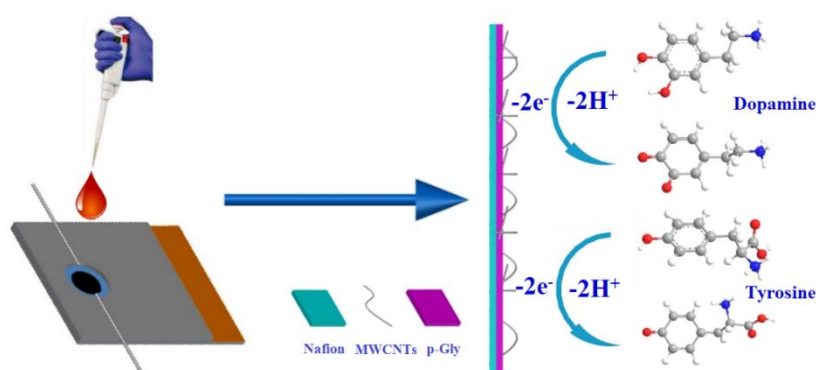
Scheme 1. The oxidation-reduction mechanism for DA and Tyr at p-Gly/Nafion/MWCNTs/CPE-PMEP.

3.4 Calibration curve and detection limit

Firstly, the LSV curves were recorded when the concentration of Tyr remained unchanged and the concentration of DA was successively increased. As shown in Fig. 7A, two well-separated and distinct oxidation peaks of DA and Tyr were observed, and there was no significant change of the LSV response of Tyr with consequence additions of DA. These demonstrate that Tyr has no interfering effect on the detection of DA. The peak current and the concentration of Tyr showed a good linear relationship at the range from 0.2-40 μM (Fig. 7B). The linear regression equation was $I_{pa, DA}$ (μA) = 3.0392c (μM) - 0.212 (R^2 = 0.997), and the detection limit was obtained as 0.008 μM (S/N=3).
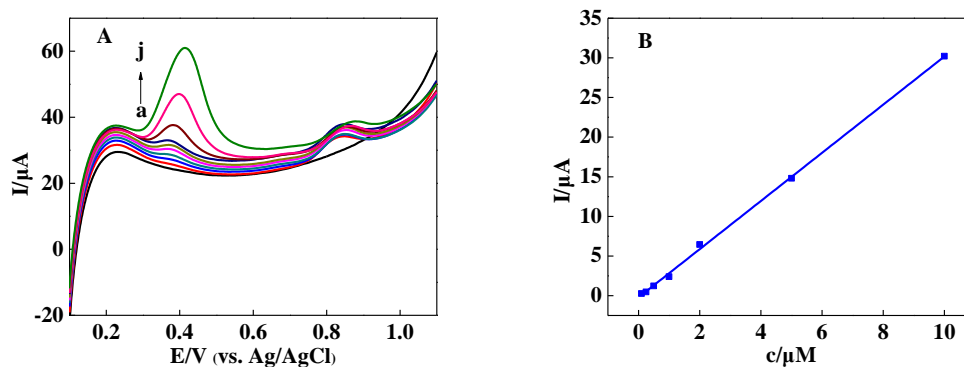
Figure 7. (A) LSV curves of successive addition of DA (a: bg, b→j: 0.025-10 μM) in the presence of 20 μM Tyr at p-Gly/Nafion/MWCNTs/CPE-PMEP (B) The linear relationship of peak current and the concentration of DA. Scan rate: 50 mV·s^{-1}, buffer solution: BRBS (pH 5.0).

Secondly, the LSV curves were recorded when the concentration of DA remained unchanged and the concentration of Tyr successively increased. As shown in Fig. 8A, two well-separated and distinct oxidation peaks of DA and Tyr were observed, and there was no significant change of the LSV response of DA with consequence additions of Tyr. These demonstrate that DA has no interfering effect on the detection of Tyr. The peak current and the concentration of Tyr showed a good linear relationship at the range from 0.2-40 μM (Fig. 8B). The linear regression equation was $I_{pa, Tyr}$ (μA) = 0.287c (μM) - 0.002 (R^2 = 0.998), and the detection limit was obtained as 0.07 μM (S/N=3).
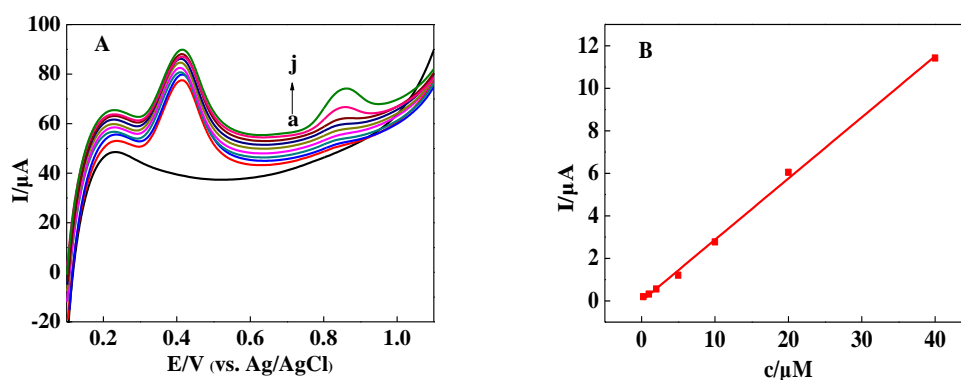
Figure 8. (A) LSV curves of successive addition of Tyr (a: bg, b→j: 0.2-40 μM) in the presence of 5 μM Tyr at p-Gly/Nafion/MWCNTs/CPE-PMEP. (B) The linear relationship of peak current and the concentration of Tyr. Scan rate: 50 mV·s^{-1}, buffer solution: BRBS (pH 5.0).

3.5 Reproducibility and stability of p-Gly/Nafion/MWCNTs/CPE-PMEP

To evaluate the reproducibility and stability of the sensor, five p-Gly/Nafion/MWCNTs/CPE-PMEPs were fabricated individually by the same procedure and used for the simultaneous detection of 10 μM DA and 30 μM Tyr (Fig.9). The relative standard deviation (RSD) of DA or Tyr oxidation peak currents were less than or equal to 3.1%. The sensor retained 85% of the initial current response value after storage at 4 °C for two weeks. These results proved that p-Gly/Nafion/MWCNTs/CPE-PMEP

possesses acceptable reproducibility and stability.
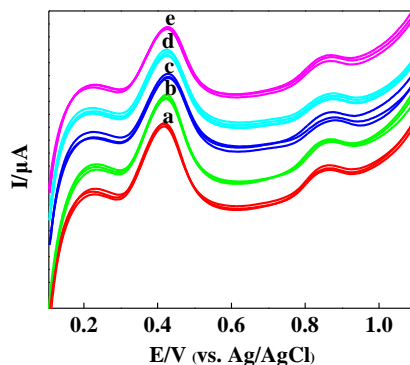
Figure 9. LSV curves of different p-Gly/Nafion/MWCNTs/CPE-PMEPs (n = 5) (a→e: No. 1- No.5) in BRBS (pH 5.0) containing 10 µM DA and 30 µM Tyr, scan rate: 50 mV·s⁻¹.

3.6 Comparison between p-Gly/Nafion/MWCNTs/CPE-PMEP *and other sensors*

The comparison between the analytical performance of the reported method and previously reported methods of electrochemical determination of DA and Tyr is given in Table 1. The data reveals that p-Gly/Nafion/MWCNTs/CPE-PMEP shows superior analytical performance in terms of linear dynamic range and low detection limit over methods using other chemically modified electrodes reported in literatures.

Table 1. Comparison between the proposed sensor and other sensors for DA and Tyr assays.

Electrode	Target Molecule	Linear range (µM)	LOD (µM)	Ref.
AuNPs/MWCNTs/GCE	Tyr	0.4-80	0.2	[33]
AuNPs/poly(trisamine)/GCE	Tyr	3.9-61.8	0.9	[34]
AuNPs/PTAT/GCE	Tyr	10-560	2	[35]
PbO₂/ carbon ceramic electrode(CCE)	Tyr	5-1458	0.77	[36]
AuNPs/Trp-GR/GCE	DA	0.5-411	0.056	[37]
Py-PBA/GCE	DA	0.05-10	0.033	[38]
PPy/ZIF-67/MIPs/ Nafion/GCE	DA	0.08-50	0.031	[39]
AuNPs/GR/OPPy/GCE	DA	0.5-8	0.1	[40]
Iron(III) Doped Zeolite/CPE	DA	0.1-200	0.05	
	Tyr	0.5-200	0.08	[41]
Porphyrin-clay/CPE	DA	0.4-10.3	0.1	
	Tyr	3-51	0.7	[42]
GR nanowalls/Ta	DA	0.2-10	0.04	
	Tyr	3-200	0.6	[43]
p-Gly/Nafion/MWCNTs/ CPE-PMEP	DA	0.025-10	0.008	
	Tyr	0.2-40	0.07	This work

3.7 Quantification of DA and Tyr in human serum samples

Under the optimized experimental conditions, the simultaneous detection of DA and Tyr in human serum samples was performed at p-Gly/Nafion/MWCNTs/CPE-PMEP. As shown in Table 2, the recoveries for DA and Tyr are from 92.0% to 99.8% (RSD≤3.1) and 96.5% to 100.5% (RSD≤3.0), respectively. These results indicate that the presented sensor is reliable for simultaneous determination of DA and Tyr in real human serum samples.

Table 2. Analytical results for DA and Tyr in human serum samples (n = 5).

Added/(µM)		Determined/(µM)		Recovery/%		RSD/%	
DA	Tyr	DA	Tyr	DA	Tyr	DA	Tyr
0	0	0.47	1.38	/	/	2.7	3.0
1	2	1.39	3.31	92.0	96.5	3.1	2.8
2	5	2.36	6.39	94.5	100.2	3.0	2.9
5	10	5.46	11.43	99.8	100.5	2.4	2.7

4. CONCLUSION

In summary, the electrochemical sensor based on p-Gly/Nafion/MWCNTs functionalized PMEP has been fabricated for simultaneous determination of DA and Tyr. The proposed method showed high sensitivity and selectivity. What's more, p-Gly/Nafion/MWCNTs/CPE-PMEP has used for the detection of DA and Tyr in human serum samples. The results demonstrated that p-Gly/Nafion/MWCNTs/CPE-PMEP is feasible for DA and Tyr detection in practical samples.

References

1. L. Garcia-Carmona, M. Moreno-Guzman, T. Sierra, M. C. Gonzalez and A. Escarpa, *Sens. Actuat. B-Chem.,* 259(2018)762-767.
2. P. J. Asiello and A. J. Baeumner, *Lab on a Chip,* 11(2011)1420-1430.
3. W. Gao, S. Emaminejad, H. Y. Y. Nyein, S. Challa, K. V. Chen, A. Peck, H. M. Fahad, H. Ota, H. Shiraki, D. Kiriya, D. H. Lien, G. A. Brooks, R. W. Davis and A. Javey, *Nature,* 529(2016)509-+.
4. B. K. Paul, A. K. Panigrahi, V. Singh and S. G. Singh, *Acs Appl. Mater. Inter.,* 9(2017)39994-40005.
5. L. Backman, U. Lindenberger, S. C. Li and L. Nyberg, *Neurosci. Biobehav. R.,* 34(2010)670-677.
6. L. F. Burbulla, P. P. Song, J. R. Mazzulli, E. Zampese, Y. C. Wong, S. Jeon, D. P. Santos, J. Blanz, C. D. Obermaier, C. Strojny, J. N. Savas, E. Kiskinis, X. X. Zhuang, R. Kruger, D. J. Surmeier and D. Krainc, *Science,* 357(2017)1255-+.
7. O. D. Howes, A. J. Montgomery, MC. Asselin, R. M. Murray, I. Valli, P. Tabraham, E. Bramon-Bosch, L. Valmaggia, L. Johns, M. Broome, P. K. McGuire and P. M. Grasby, *Arch. Gen. Psychiat.,* 66(2009)13-20.
8. H. S. Singer, S. Szymanski, J. Giuliano, F. Yokoi, A. S. Dogan, J. R. Brasic, Y. Zhou, A. A. Grace and D. F. Wong, *Am. J. Psychiat.,* 159(2002)1329-1336.
9. M. Rios, B. Habecker, T. Sasaoka, G. Eisenhofer, H. Tian, S. Landis, D. Chikaraishi and S. Roffler-Tarlov, *J. Neurosci.,* 19(1999)3519-3526.
10. M. K. Hostetter, H. L. Levy, H. S. Winter, G. J. Knight and J. E. Haddow, *New Engl. J. Med.,* 308(1983)1265-1267.
11. C. Lin, Y. C. Jair, Y. C. Chou, P. S. Chen and Y. C. Yeh, *Anal. Chim. Acta,* 1041(2018)108-113.

12. C. Ramdani, F. Vidal, A. Dagher, L. Carbonnell and T. Hasbroucq, *Psychopharmacology,* 235(2018)1307-1316.
13. D. Wu, H. Xie, H. F. Lu, W. Li and Q. L. Zhang, *Biomed. Chromatogr.,* 30(2016)1458-1466.
14. X. M. Mo, Y. Li, A. G. Tang and Y. P. Ren, *Clin. Biochem.,* 46(2013)1074-1078.
15. Y. Y. Hu, X. Wu, Y. Y. Su, X. D. Hou and J. Y. Zhang, *Microchim. Acta,* 166(2009)289-294.
16. Y. Huang, X.Y. Jiang, W. Wang, J. P. Duan and G. N. Chen, *Talanta,* 70(2006)1157-1163.
17. R. P. Ribeiro, J. C. Gasparetto, R. D. Vilhena, T. M. G. de Francisco, C. A. F. Martins, M. A. Cardoso, R. Pontarolo and K. A. T. de Carvalho, *Bioanalysis,* 7(2015)207-220.
18. H. Yoshida, T. Mizukoshi, K. Hirayama and H. Miyano, *J. Agr. Food Chem.,* 55(2007)551-560.
19. K. Jackowska and P. Krysinski, *Anal. Bioanal. Chem.,* 405(2013)3753-3771.
20. M. Sajid, M. K. Nazal, M. Mansha, A. Alsharaa, S. M. S. Jillani and C. Basheer, *Trac-Trend Anal. Chem.,* 76(2016)15-29.
21. M. M. Rahman, N. S. Lopa, K. Kim and J. J. Lee, *J. Electroanal. Chem.,* 754(2015)87-93.
22. A. Afkhami, F. Kafrashi, T. Madrakian, *Ionics,* 21(2015)2937-2947.
23. B. G. Mahmoud, M. Khairy, F. A. Rashwan and C. E. Banks, Anal. Chem., 89(2017)2170-2178.
24. S. Kumar, R. Rani, N. Dilbaghi, K. Tankeshwar and K. H. Kim, *Chem. Soc. Rev.,* 46(2017)158-196.
25. B. J. Zhang, L. M. Huang, M. H. Tang, K. W. Hunter, Y. Feng, Q. W. Sun, J. K. Wang and G. S. Chen, *Microchim. Acta,* 185(2018)
26. T. Thomas, R. J. Mascarenhas, B. E. K. Swamy, P. Martis, Z. Mekhalif and B. S. Sherigara, *Colloid Surface B,* 110(2013)458-465.
27. X. C. Li, Z. G. Chen, Y. W. Zhong, F. Yang, J. B. Pan and Y. J. Liang, *Anal. Chim. Acta,* 710(2012)118-124.
28. Z. Q. Wei, Y. J. Sun, Q. W. Yin, L. X. Wang, S. G. Chen, R. Sheng, D. Y. Pan, H. Yang and S. Q. Li, *Int. J. Electrochem. Sci.,* 13(2018)7478-7488.
29. Y. M. Yang, J. Liu, S. J. Guo, Y. Liu and Z. H. Kang, *J. Mater. Chem. A,* 3(2015)18598-18604.
30. Z. Q. Wei, S. F. Guo, L. Y. Cheng, T. Li, Y. L. Zhang and H. Yang, *Int. J. Electrochem. Sci.,* 14(2019)6748-6758.
31. H. Yang, Z.Q. Wei, S.N. He, T. Li, Y. F. Zhu, L. X. Duan, Y. Li and J. G. Wang, *Int. J. Electrochem. Sci.,* 12(2017) 11089-11101.
32. H. R. Zare, B. Moradiyan, Z. Shekari and A. Benvidi, *Measurement,* 90(2016)510-518.
33. T. Madrakian, E. Haghshenas and A. Afkhami, *Sens. Actuat. B-Chem.,* 193(2014)451-460.
34. M. Taei and G. Ramazani, *Colloid Surface B,* 123(2014)23-32.
35. M. Taei, F. Hasanpour, H. Salavati, S. H. Banitaba and F. Kazemi, *Mat. Sci. Eng. C-Mater.,* 59(2016)120-128.
36. H. Heidari and E. Habibi, *J. Iran. Chem. Soc.,* 15(2018)885-892.
37. Q. W. Lian, A. Luo, Z. Z. An, Z. Li, Y. Y. Guo, D. X. Zhang, Z. H. Xue, X. B. Zhou and X. Q. Lu, *Appl. Surf. Sci.,* 349(2015)184-189.
38. M. Zhong, Y. Teng, S. F. Pang, L. Q. Yan and X. W. Kan, *Biosens. Bioelectron.,* 64(2015)212-218.
39. W. Q. Zhang, D. W. Duan, S. Q. Liu, Y. S. Zhang, L. P. Leng, X. L. Li, N. Chen and Y. P. Zhang, *Biosens. Bioelectron,* 118(2018)129-136.
40. D. P. Tuyen, D. P. Quan, N. H. Binh, V. C. Nguyen, T. D. Lam, L. T. Huyen, L. H. Nguyen, P. H. Viet, N. T. Loc and T. Q. Huy, *J. Mol. Liq.,* 198(2014)307-312.
41. A. Babaei, M. Zendehdel, B. Khalilzadeh and M. Abnosi, *Chinese J. Chem.,* 28(2010)1967-1972.
42. J. C. Kemmegne-Mbouguen and E. Ngameni, *Anal. Methods-Uk,* 9(2017)4157-4166.
43. F. Y. Tian, H. J. Li, M. J. Li, C. P. Li, Y. J. Lei and B. H. Yang, *Microchim. Acta,* 184(2017)1611-1619.